

**ADSORPTION OF Cu(II) AND Ni(II) IONS USING  
CHITOSAN-BENZALDEHYDE BEADS**

**LAW SHUN CHIN**

**UNIVERSITI SAINS MALAYSIA**

**2016**

**ADSORPTION OF Cu(II) AND Ni(II) IONS USING  
CHITOSAN-BENZALDEHYDE BEADS**

**by**

**LAW SHUN CHIN**

**Thesis submitted in fulfillment of the requirements  
for the degree of Master of Science**

**May 2016**

## ACKNOWLEDGEMENT

I would like to express my deepest special appreciations and thanks to my supervisor Professor Wan Saime Wan Ngah, for helping me solved the problems that I had encountered during my research. The advices and the encouragements given are priceless for me. I would also like to thanks the Kementerian Pendidikan Malaysia MyBrain 15 for the financial support throughout my research.

Special thanks are given to the lab assistant, Puan Saripah and Mr. Marimuthu as they give a lot of assists in technical support and the guidance during the samples testing and data collection by using the FTIR spectroscopy.

My sincere thanks also go to my friends, Ms. Yeoh Kim Hoey, Ms. Teong Lee Ching, Ms. Fatin and Mr. Toh Run Hong for their brilliant suggestion and comments during my research.

Last but not the least, I would like to thanks my lovely parents (Mr. Law Chan Yue and Mrs. Wong Kuan Chin), elder brother (Mr. Law Kim Hee) and two younger brothers (Mr. Law Kah Hee and Mr. Law Lin Hee) for their mentally and physically supports. Their prayer for me was what sustained me thus far.

Thank you.

## TABLE OF CONTENTS

	<b>Page</b>
<b>ACKNOWLEDGEMENT</b>	ii
<b>TABLE OF CONTENTS</b>	iii
<b>LIST OF TABLES</b>	viii
<b>LIST OF FIGURES</b>	x
<b>LIST OF ABBREVIATIONS AND SYMBOLS</b>	xv
<b>ABSTRAK</b>	xviii
<b>ABSTRACT</b>	xx
<b>CHAPTER ONE-INTRODUCTION</b>	
1.1 Heavy Metals in Our Environment	1
1.1.1 Copper	1
1.1.2 Nickel	3
1.2 Treatment Technology for Heavy Metals Containing Wastewater	5
1.2.1 Chemical precipitation	6
1.2.2 Ion exchange technique	8
1.2.3 Membrane separation	9
1.2.4 Electrocoagulation	12
1.2.5 Electroflotation	13
1.2.6 Adsorption technique	14
1.3 Chitin	19
1.3.1 Source of chitin	19
1.3.2 Propertise of chitin	20
1.4 Chitosan	21

1.4.1	Propertise of chitosan	21
1.5	Application of Chitosan	22
1.5.1	Textile industry	22
1.5.2	Food industry	24
1.5.3	Agriculture industry	25
1.5.4	Medical	26
1.5.5	Wastewater treatment	27
1.6	Modification of Chitosan	29
1.6.1	Physical modification	29
1.6.2	Chemical modification	30
1.7	Research Objective	34

## **CHAPTER TWO - MATERIALS AND METHODS**

2.1	List of Chemicals and Instruments	35
2.1.1	Chemicals	35
2.1.2	Instruments	36
2.2	Determination of the Degree of Deacetylation of Chitosan	36
2.3	Preparation of Chitosan Beads	37
2.4	Preparation of Chitosan-Benzaldehyde Beads	39
2.5	Preparation of Stock Solution	41
2.5.1	Stock solution of 1000 mg/L Cu <sup>2+</sup> ions	41
2.5.2	Stock solution of 1000 mg/L Ni <sup>2+</sup> ions	41
2.6	Characterization of Chitosan, Chitosan-benzaldehyde 1:1 and 1:2 Beads	42
2.6.1	Fourier transform infrared spectroscopy (FTIR)	42
2.6.2	Surface area and pore analysis	42

2.6.3	Scanning electron microscopy (SEM) and energy dispersive X-ray (EDX) analyzer	42
2.6.4	Determination of point of zero charge ( $\text{pH}_{\text{pzc}}$ )	43
2.6.5	Dissolution and swelling test	43
2.7	Batch Adsorption Experiments	44
2.7.1	Determination of precipitation pH of $\text{Cu}^{2+}$ and $\text{Ni}^{2+}$ hydroxide	45
2.7.2	Determination of optimum pH	46
2.7.3	Determination of optimum contact time	46
2.7.4	Determination of optimum agitation rate	47
2.7.5	Determination of optimum adsorbent dosage	48
2.7.6	Effect of initial concentration and contact time	48
2.8	Isotherm Studies	49
2.8.1	Determination of precision for adsorption studies	50
2.9	Fixed Bed Column Experiment	51
2.10	Adsorption-Desorption Study	52

### **CHAPTER THREE–RESULTS AND DISCUSSIONS**

3.1	Degree of Deacetylation of Chitosan	54
3.2	Preparation and Characterization of Chitosan Beads	55
3.3	Preparation and Characterization of Chitosan-benzaldehyde 1:1 and 1:2 Beads	57
3.3.1	Fourier transform infrared spectroscopy (FTIR)	59
3.3.2	Surface area and pore analysis	63
3.3.3	Scanning electron microscopy (SEM) and energy dispersive X-ray (EDX) analyzer	64

3.3.4	Determination of point of zero charge ( $\text{pH}_{\text{zpc}}$ )	66
3.3.5	Dissolution and swelling test for chitosan-benzaldehyde 1:1 and 1:2 beads	68
3.4	Adsorption of $\text{Cu}^{2+}$ and $\text{Ni}^{2+}$ Ions onto Chitosan-benzaldehyde 1:1 and 1:2 Beads	70
3.4.1	Determination of $\text{Cu}^{2+}$ and $\text{Ni}^{2+}$ hydroxide formation	70
3.4.2	Effect of initial pH on the adsorption of $\text{Cu}^{2+}$ and $\text{Ni}^{2+}$ ions onto chitosan-benzaldehyde 1:1 and 1:2 beads	72
3.4.3	Effect of contact time on the adsorption of $\text{Cu}^{2+}$ and $\text{Ni}^{2+}$ ions onto chitosan-benzaldehyde 1:1 and 1:2 beads	74
3.4.4	Effect of agitation rate on the adsorption of $\text{Cu}^{2+}$ and $\text{Ni}^{2+}$ ions onto chitosan-benzaldehyde 1:1 and 1:2 beads	76
3.4.5	Effect of adsorbent dosage on the adsorption of $\text{Cu}^{2+}$ and $\text{Ni}^{2+}$ ions onto chitosan-benzaldehyde 1:1 and 1:2 beads	78
3.4.6	Effect of initial concentration and contact time	82
3.5	Adsorption Kinetic	85
3.5.1	Pseudo-first order kinetic model	85
3.5.2	Pseudo-second order kinetic model	89
3.5.3	Intraparticle diffusion model	94
3.5.4	Elovich model	98
3.6	Adsorption Isotherm	102
3.6.1	Effect of initial concentration on the adsorption of $\text{Cu}^{2+}$ and $\text{Ni}^{2+}$ ions onto chitosan-benzaldehyde 1:1 and 1:2 beads	102
3.6.2	Langmuir isotherm model	105
3.6.3	Freundlich isotherm model	109

3.6.4	Dubinin–Radushkevich (D-R) isotherm model	112
3.6.5	Redlich-Peterson (R-P) isotherm model	115
3.7	Thermodynamic of the Adsorption Process	118
3.8	Determination of Precision for Adsorption Studies	123
3.9	Fixed Bed Column Study	124
3.9.1	Adam-Bohart model	130
3.9.2	Thomas model	134
3.9.3	Yoon-Nelson model	138
3.10	Adsorption-Desorption Study	142
<b>CHAPTER FOUR – CONCLUSIONS</b>		144
<b>CHAPTER FIVE-RECOMMENDATIONS FOR FUTURE RESEARCH</b>		147
<b>REFERENCES</b>		148

## LIST OF TABLES

		<b>Page</b>
Table 1.1	Summary of type of natural adsorbents used in removal of heavy metal	16
Table 1.2	Examples of modified chitosan and the maximum adsorption of different metal ions.	32
Table 3.1	Summary of infrared adsorption band for chitosan beads	56
Table 3.2	Summary of infrared adsorption band for chitosan-benzaldehyde 1:1 beads	59
Table 3.3	BET surface area and average pore diameter for chitosan-benzaldehyde 1:1 and 1:2 beads	63
Table 3.4	Dissolution effect of chitosan-benzaldehyde 1:1 and 1:2 beads indifferent medium	69
Table 3.5	Percentage of swelling of chitosan-benzaldehyde 1:1 and 1:2 beads in different medium	69
Table 3.6	Pseudo-first order kinetic model constants and correlation coefficient, $R^2$ for the adsorption of $Cu^{2+}$ ions onto chitosan-benzaldehyde 1:1 and 1:2 beads at different initial concentration	88
Table 3.7	Pseudo-first order kinetic model constants and correlation coefficient, $R^2$ for the adsorption of $Ni^{2+}$ ions onto chitosan-benzaldehyde 1:1 and 1:2 beads at different initial concentration	89
Table 3.8	Pseudo-second order kinetic model constants and correlation coefficient, $R^2$ for the adsorption of $Cu^{2+}$ ions onto chitosan-benzaldehyde 1:1 and 1:2 beads at different initial concentration	93
Table 3.9	Pseudo-second order kinetic model constants and correlation coefficient, $R^2$ for the adsorption of $Ni^{2+}$ ions onto chitosan-benzaldehyde 1:1 and 1:2 beads with different initial concentration	93
Table 3.10	Intraparticle kinetic model constants and correlation coefficient, $R^2$ for the adsorption of $Cu^{2+}$ ions onto chitosan-benzaldehyde 1:1 and 1:2 beads at different initial concentration	97
Table 3.11	Intraparticle kinetic model constants and correlation coefficient, $R^2$ for the adsorption of $Ni^{2+}$ ions onto chitosan-benzaldehyde	98

1:1 and 1:2 beads with different initial concentration

Table 3.12	Elovich kinetic model constants and correlation coefficient, $R^2$ for the adsorption of $\text{Cu}^{2+}$ ions onto chitosan-benzaldehyde 1:1 and 1:2 beads at different initial concentration	101
Table 3.13	Elovich kinetic model constants and correlation coefficient, $R^2$ for the adsorption of $\text{Ni}^{2+}$ ions onto chitosan-benzaldehyde 1:1 and 1:2 beads at different initial concentration	102
Table 3.14	Langmuir isotherm parameters and correlation coefficients, $R^2$ of $\text{Cu}^{2+}$ and $\text{Ni}^{2+}$ ions for chitosan-benzaldehyde 1:1 and 1:2 beads at 300 K	109
Table 3.15	Freundlich isotherm parameters and correlation coefficients, $R^2$ of $\text{Cu}^{2+}$ and $\text{Ni}^{2+}$ ions for chitosan-benzaldehyde 1:1 and 1:2 beads at 300 K	112
Table 3.16	Dubinin–Radushkevich isotherm parameters and correlation coefficients, $R^2$ of $\text{Cu}^{2+}$ and $\text{Ni}^{2+}$ ions for chitosan-benzaldehyde 1:1 and 1:2 beads at 300 K	115
Table 3.17	R-P isotherm constants isotherm parameters and correlation coefficients, $R^2$ of $\text{Cu}^{2+}$ and $\text{Ni}^{2+}$ ions for chitosan-benzaldehyde 1:1 and 1:2 beads at 300 K	118
Table 3.18	Thermodynamic parameters for the adsorption of $\text{Cu}^{2+}$ and $\text{Ni}^{2+}$ ions for chitosan-benzaldehyde 1:1 and 1:2 beads	122
Table 3.19	The breakthrough parameters of $\text{Cu}^{2+}$ and $\text{Ni}^{2+}$ ions adsorption onto chitosan-benzaldehyde 1:1 and 1:2 beads	129
Table 3.20	Adam-Bohart model parameters at different initial concentration of $\text{Cu}^{2+}$ and $\text{Ni}^{2+}$ ions and correlation coefficient, $R^2$ for chitosan-benzaldehyde 1:1 and 1:2 beads	133
Table 3.21	Thomas model parameters at different initial concentration of $\text{Cu}^{2+}$ and $\text{Ni}^{2+}$ ions and correlation coefficient, $R^2$ for chitosan-benzaldehyde 1:1 and 1:2 beads	137
Table 3.22	Yoon-Nelson model parameters at different initial concentration of $\text{Cu}^{2+}$ and $\text{Ni}^{2+}$ ions and correlation coefficient, $R^2$ for chitosan-benzaldehyde 1:1 and 1:2 beads	142
Table 3.23	Percentage of desorption of $\text{Cu}^{2+}$ and $\text{Ni}^{2+}$ ions using different concentration of $\text{Na}_2\text{EDTA}$ solutions.	143

## LIST OF FIGURES

		<b>Page</b>
Figure 1.1	Structures of chitin, cellulose and chitosan (Krajewska, 2004)	20
Figure 2.1	Schematic diagram on the preparation of chitosan beads	38
Figure 2.2	Schematic diagram on the preparation of chitosan-benzaldehyde 1:1 and 1:2 beads	40
Figure 2.3	Experimental set up for fixed bed operations	52
Figure 3.1	FTIR spectra of chitosan bead	56
Figure 3.2	FTIR spectra of chitosan-benzaldehyde 1:1 and 1:2 beads	58
Figure 3.3	Scheme for the synthesis of the chitosan-benzaldehyde beads	59
Figure 3.4	FTIR spectra of chitosan-benzaldehyde 1:1 beads before and after loading with $\text{Cu}^{2+}$ and $\text{Ni}^{2+}$ ions	61
Figure 3.5	FTIR spectra of chitosan-benzaldehyde 1:2 beads before and after loading with $\text{Cu}^{2+}$ and $\text{Ni}^{2+}$ ions	62
Figure 3.6	Proposed mechanism of chitosan-metal complex (Benavente, 2008)	62
Figure 3.7	SEM-EDX micrograph obtained for chitosan-benzaldehyde 1:1 beads (x 1000)	65
Figure 3.8	SEM-EDX micrograph obtained for chitosan-benzaldehyde 1:2 beads (x 1000)	65
Figure 3.9	$\text{pH}_{\text{zpc}}$ for chitosan-benzaldehyde 1:1 beads	67
Figure 3.10	$\text{pH}_{\text{zpc}}$ for chitosan-benzaldehyde 1:2 beads	67
Figure 3.11	Effect of pH on the formation of $\text{Cu}(\text{OH})_2$	71
Figure 3.12	Effect of pH on the formation of $\text{Ni}(\text{OH})_2$	71
Figure 3.13	Effect of pH on the adsorption of $\text{Cu}^{2+}$ ions onto chitosan-benzaldehyde 1:1 and 1:2 beads	73
Figure 3.14	Effect of pH on the adsorption of $\text{Ni}^{2+}$ ions onto chitosan-benzaldehyde 1:1 and 1:2 beads	74
Figure 3.15	Effect of contact time on the adsorption of $\text{Cu}^{2+}$ ions onto	75

	chitosan-benzaldehyde 1:1 and 1:2 beads	
Figure 3.16	Effect of contact time on the adsorption of Ni <sup>2+</sup> ions onto chitosan-benzaldehyde 1:1 and 1:2 beads	76
Figure 3.17	Effect of agitation rate on the adsorption of Cu <sup>2+</sup> ions onto chitosan-benzaldehyde 1:1 and 1:2 beads	77
Figure 3.18	Effect of agitation rate on the adsorption of Ni <sup>2+</sup> ions onto chitosan-benzaldehyde 1:1 and 1:2 beads	77
Figure 3.19	Effect of adsorbent dosage on the adsorption of Cu <sup>2+</sup> ions onto chitosan-benzaldehyde 1:1 beads	80
Figure 3.20	Effect of adsorbent dosage on the adsorption of Cu <sup>2+</sup> ions onto chitosan-benzaldehyde 1:2 beads	80
Figure 3.21	Effect of adsorbent dosage on the adsorption of Ni <sup>2+</sup> ions onto chitosan-benzaldehyde 1:1 beads	81
Figure 3.22	Effect of adsorbent dosage on the adsorption of Ni <sup>2+</sup> ions onto chitosan-benzaldehyde 1:2 beads	81
Figure 3.23	Effect of concentration with contact time on the adsorption of Cu <sup>2+</sup> ions onto chitosan-benzaldehyde 1:1 beads	82
Figure 3.24	Effect of concentration with contact time on the adsorption of Cu <sup>2+</sup> ions onto chitosan-benzaldehyde 1:2 beads	83
Figure 3.25	Effect of concentration with contact time on the adsorption of Ni <sup>2+</sup> ions onto chitosan-benzaldehyde 1:1 beads	83
Figure 3.26	Effect of concentration with contact time on the adsorption of Ni <sup>2+</sup> ions onto chitosan-benzaldehyde 1:2 beads	84
Figure 3.27	Pseudo-first order plot for the adsorption of Cu <sup>2+</sup> ions onto chitosan-benzaldehyde 1:1 beads	86
Figure 3.28	Pseudo-first order plot for the adsorption of Cu <sup>2+</sup> ions onto chitosan-benzaldehyde 1:2 beads	87
Figure 3.29	Pseudo-first order plot for the adsorption of Ni <sup>2+</sup> ions onto chitosan-benzaldehyde 1:1 beads	87
Figure 3.30	Pseudo-first order plot for the adsorption of Ni <sup>2+</sup> ions onto chitosan-benzaldehyde 1:2 beads	88
Figure 3.31	Pseudo-second order plot for the adsorption of Cu <sup>2+</sup> ions onto chitosan-benzaldehyde 1:1 beads	90

Figure 3. 32	Pseudo-second order plot for the adsorption of $\text{Cu}^{2+}$ ions onto chitosan-benzaldehyde 1:2 beads	91
Figure 3. 33	Pseudo-second order plot for the adsorption of $\text{Ni}^{2+}$ ions onto chitosan-benzaldehyde 1:1 beads	91
Figure 3. 34	Pseudo-second order plot for the adsorption of $\text{Ni}^{2+}$ ions onto chitosan-benzaldehyde 1:2 beads	92
Figure 3. 35	Intraparticle diffusion plot for the adsorption of $\text{Cu}^{2+}$ ions onto chitosan-benzaldehyde 1:1 beads	95
Figure 3. 36	Intraparticle diffusion plot for the adsorption of $\text{Cu}^{2+}$ ions onto chitosan-benzaldehyde 1:2 beads	96
Figure 3. 37	Intraparticle diffusion plot for the adsorption of $\text{Ni}^{2+}$ ions onto chitosan-benzaldehyde 1:1 beads	96
Figure 3. 38	Intraparticle diffusion plot for the adsorption of $\text{Ni}^{2+}$ ions onto chitosan-benzaldehyde 1:2 beads	97
Figure 3. 39	Elovich plot for the adsorption of $\text{Cu}^{2+}$ ions onto chitosan-benzaldehyde 1:1 beads	99
Figure 3. 40	Elovich plot for the adsorption of $\text{Cu}^{2+}$ ions onto chitosan-benzaldehyde 1:2 beads	100
Figure 3. 41	Elovich plot for the adsorption of $\text{Ni}^{2+}$ ions onto chitosan-benzaldehyde 1:1 beads	100
Figure 3. 42	Elovich plot for the adsorption of $\text{Ni}^{2+}$ ions onto chitosan-benzaldehyde 1:2 beads	101
Figure 3. 43	Equilibrium adsorption isotherm for the adsorption of $\text{Cu}^{2+}$ ions onto chitosan-benzaldehyde 1:1 and 1:2 beads	103
Figure 3. 44	Equilibrium adsorption isotherm for the adsorption of $\text{Ni}^{2+}$ ions onto chitosan-benzaldehyde 1:1 and 1:2 bead	104
Figure 3. 45	Non-linear Langmuir isotherm for the adsorption of $\text{Cu}^{2+}$ ions onto chitosan-benzaldehyde 1:1 and 1:2 beads	107
Figure 3. 46	Non-linear Langmuir isotherm for the adsorption of $\text{Ni}^{2+}$ ions onto chitosan-benzaldehyde 1:1 and 1:2 beads	108
Figure 3. 47	$R_L$ plot of $\text{Cu}^{2+}$ and $\text{Ni}^{2+}$ ions onto chitosan-benzaldehyde 1:1 and 1:2 beads	108
Figure 3. 48	Non-linear Freundlich isotherm for the adsorption of $\text{Cu}^{2+}$ ions onto chitosan-benzaldehyde 1:1 and 1:2 beads	111

Figure 3. 49	Non-linear Freundlich isotherm for the adsorption of Ni <sup>2+</sup> ions onto chitosan-benzaldehyde 1:1 and 1:2 beads	111
Figure 3. 50	Non-linear Dubinin–Radushkevich isotherm for the adsorption of Cu <sup>2+</sup> ions onto chitosan-benzaldehyde 1:1 and 1:2 beads	114
Figure 3. 51	Non-linear Dubinin–Radushkevich isotherm for the adsorption of Ni <sup>2+</sup> ions onto chitosan-benzaldehyde 1:1 and 1:2 beads	114
Figure 3. 52	Non-linear Redlich-Peterson isotherm for the adsorption of Cu <sup>2+</sup> ions onto chitosan-benzaldehyde 1:1 and 1:2 beads	117
Figure 3. 53	Non-linear Redlich-Peterson isotherm for the adsorption of Ni <sup>2+</sup> ions onto chitosan-benzaldehyde 1:1 and 1:2 beads	117
Figure 3. 54	van't Hoff plot for the adsorption of Cu <sup>2+</sup> ions onto chitosan-benzaldehyde 1:1 beads	120
Figure 3. 55	van't Hoff plot for the adsorption of Cu <sup>2+</sup> ions onto chitosan-benzaldehyde 1:2 beads	121
Figure 3. 56	van't Hoff plot for the adsorption of Ni <sup>2+</sup> ions onto chitosan-benzaldehyde 1:1 beads	121
Figure 3. 57	van't Hoff plot for the adsorption of Ni <sup>2+</sup> ions onto chitosan-benzaldehyde 1:2 beads	122
Figure 3. 58	Typical breakthrough profile from a column study (Ahamad and Jawed, 2011a)	125
Figure 3. 59	Breakthrough curve for the adsorption of Cu <sup>2+</sup> ions onto chitosan-benzaldehyde 1:1 beads	127
Figure 3. 60	Breakthrough curve for the adsorption of Cu <sup>2+</sup> ions onto chitosan-benzaldehyde 1:2 beads	128
Figure 3. 61	Breakthrough curve for the adsorption of Ni <sup>2+</sup> ions onto chitosan-benzaldehyde 1:1 beads	128
Figure 3. 62	Breakthrough curve for the adsorption of Ni <sup>2+</sup> ions onto chitosan-benzaldehyde 1:2 beads	129
Figure 3. 63	Adam-Bohart plot for the adsorption of Cu <sup>2+</sup> ions onto chitosan-benzaldehyde 1:1 beads	131
Figure 3. 64	Adam-Bohart plot for the adsorption of Cu <sup>2+</sup> ions onto chitosan-benzaldehyde 1:2 beads	132

Figure 3. 65	Adam-Bohart plot for the adsorption of Ni <sup>2+</sup> ions onto chitosan-benzaldehyde 1:1 beads	132
Figure 3. 66	Adam-Bohart plot for the adsorption of Ni <sup>2+</sup> ions onto chitosan-benzaldehyde 1:2 beads	133
Figure 3. 67	Thomas plot for the adsorption of Cu <sup>2+</sup> ions onto chitosan-benzaldehyde 1:1 beads	135
Figure 3. 68	Thomas plot for the adsorption of Cu <sup>2+</sup> ions onto chitosan-benzaldehyde 1:2 beads	136
Figure 3. 69	Thomas plot for the adsorption of Ni <sup>2+</sup> ions onto chitosan-benzaldehyde 1:1 beads	146
Figure 3. 70	Thomas plot for the adsorption of Ni <sup>2+</sup> ions onto chitosan-benzaldehyde 1:2 beads	137
Figure 3. 71	Yoon-Nelson plot for the adsorption of Cu <sup>2+</sup> ions onto chitosan-benzaldehyde 1:1 beads	140
Figure 3. 72	Yoon-Nelson plot for the adsorption of Cu <sup>2+</sup> ions onto chitosan-benzaldehyde 1:2 beads	140
Figure 3. 73	Yoon-Nelson plot for the adsorption of Ni <sup>2+</sup> ions onto chitosan-benzaldehyde 1:1 beads	141
Figure 3.74	Yoon-Nelson plot for the adsorption of Ni <sup>2+</sup> ions onto chitosan-benzaldehyde 1:2 bead	141

## LIST OF ABBREVIATIONS AND SYMBOLS

$n$	Freundlich constant related to adsorption intensity
$\bar{X}$	Mean
$\alpha$	Elovich initial adsorption rate (mg/g min)
$a_R$	R-P isotherm constant (mg/g) <sup>g</sup>
AAS	Atomic Absorption Spectrophotometer
$\beta$	Elovich desorption constant (g/mg)
$b_L$	Langmuir constant (L/mg)
BET	Brunauer-Emmett-Teller
$C_{ads}$	Concentration of metal ions adsorbed (mg/L)
$C_{des}$	Concentration of metal ions desorbed (mg/L)
$C_e$	Final/equilibrium concentration (mg/L)
$C_o$	Initial concentration (mg/L)
$C_t$	Effluent concentration at time t (mg/L)
D	Degree of deacetylation
$D_p$	Percentage of desorption
$\varepsilon$	Polanyi potential
E	Mean adsorption energy or the free energy (kJ/mol)
EDTA	Ethylenediaminetetraacetic acid
EDX	Energy dispersive X-ray
F	Linear velocity (cm/min)
g	Redlich-Peterson isotherm exponent
FTIR	Fourier transform infrared
$h_i$	Initial height of the adsorbent (cm)

$h_f$	Height of swollen adsorbent (cm) at time t
$k$	Constant related to sorption energy ( $\text{mol}^2/\text{kJ}^2$ )
$k_1$	Pseudo-first order rate constant (1/min)
$k_2$	Pseudo-second order rate constant ( $\text{g}/(\text{mg min})$ )
$k_{\text{int}}$	Intraparticle diffusion rate constant ( $\text{mg}/\text{g min}^{1/2}$ )
$k_{\text{AB}}$	Adam-Bohart adsorption rate constant ( $\text{L}/\text{mg min}$ )
$K_F$	Freundlich constant ( $\text{mg}/\text{g}$ )
$K_R$	Redlich-Peterson isotherm constant ( $\text{mg}/\text{g}$ )
$k_{\text{Th}}$	Thomas rate constant ( $\text{mL}/\text{min mg}$ )
$M$	Molarity of the solution ( $\text{mol}/\text{L}$ )
$N_o$	Column saturation concentration ( $\text{mg}/\text{L}$ )
$\text{pH}_{\text{PZC}}$	pH point of zero charge
$q_e$	Adsorption capacity at equilibrium ( $\text{mg}/\text{g}$ )
$q_{\text{total}}$	Total amount of metal ions adsorbed (mg)
$Q$	Volumetric flow rate ( $\text{mL min}^{-1}$ )
$Q_{\text{DR}}$	Maximum adsorption capacity based on D-R isotherm ( $\text{mg}/\text{g}$ )
$q_{e,\text{exp}}$	Experimental adsorption capacity ( $\text{mg}/\text{g}$ )
$q_{e,\text{cal}}$	Theoretical/Calculated adsorption capacity ( $\text{mg}/\text{g}$ )
$q_{\text{max}}$	Maximum adsorption capacity ( $\text{mg}/\text{g}$ )
$q_t$	Adsorption capacity at time t ( $\text{mg}/\text{g}$ )
$q_{\text{Th}}$	Theoretical adsorption capacity for Thomas model ( $\text{mg}/\text{g}$ )
$R$	Gas constant ( $8.314\text{J}/(\text{mol K})$ )
$R^2$	Correlation coefficient
$R_L$	Dimensionless separation factor
RMSE	Root of mean square error

rpm	Rotation per minute
RSD	Relative standard deviation
S	Percentage of swelling (%)
SEM	Scanning electron microscope
SD	Standard deviation
t	Time (min)
t <sub>total</sub>	Total flow time (min)
T	Temperature (K)
V	Volume (L)
W	Weight of the adsorbent (g)
$\Delta G^\circ$	Standard Gibbs free energy change (kJ/mol)
$\Delta H^\circ$	Standard Enthalpy change (kJ/mol)
$\Delta S^\circ$	Standard Entropy change (J/(mol K))
Z	Adsorbent bed depth (cm)

# **PENJERAPAN ION Cu(II) DAN Ni(II) MENGGUNAKAN MANIK KITOSAN-BENZALDEHID**

## **ABSTRAK**

Dua jenis manik kitosan terbitan, manik kitosan-benzaldehid 1:1 dan 1:2 telah disediakan untuk penjerapan ion  $\text{Cu}^{2+}$  dan  $\text{Ni}^{2+}$  daripada larutan akueus. Pencirian bagi kedua-dua manik kitosan-benzaldehid dibuat berdasarkan spektroskopi inframerah, analisis luas permukaan, saiz liang dan analisis mikroskop elektron pengimbas berganding dengan penyebaran tenaga sinar-X (SEM-EDX). Cas permukaan kitosan-benzaldehid dapat ditentukan melalui  $\text{pH}_{\text{PZC}}$ . Kajian penjerapan berkelompok dijalankan untuk mengkaji keadaan optimum bagi penyingkiran ion  $\text{Cu}^{2+}$  dan  $\text{Ni}^{2+}$  menggunakan manik kitosan-benzaldehid supaya data yang diperoleh dapat diimplementasikan dalam kajian yang seterusnya. Berdasarkan kajian termodinamik, perubahan entalpi piawai ( $\Delta H^\circ$ ) memberikan nilai positif bagi manik kitosan-benzaldehid 1:1 dan 1:2 serta menunjukkan proses endotermik. Penjerapan ion  $\text{Cu}^{2+}$  dan  $\text{Ni}^{2+}$  menunjukkan nilai korelasi yang baik untuk model kinetik tertib pseudo-kedua untuk manik kitosan-benzaldehid 1:1 dan 1:2. Data dari eksperimen paling sesuai untuk dipadankan dengan isotherma Freundlich dan Redlich-Peterson untuk manik kitosan-benzaldehid 1:1 dan 1:2. Penjerapan maksimum bagi ions  $\text{Cu}^{2+}$  adalah masing-masing 81.76 and 55.53 mg/g bagi manik kitosan-benzaldehid 1:1 dan 1:2 manakala penjerapan maksimum bagi ions  $\text{Ni}^{2+}$  adalah masing-masing 30.34 dan 20.42 mg/g bagi manik kitosan-benzaldehid 1:1 dan 1:2. Bagi kajian penjerapan secara terus terpadat, data eksperimen menuruti model Thomas dan model Yoon-Nelson untuk kedua-dua manik kitosan-benzaldehid 1:1 dan 1:2. Peratus

penyahjerapan adalah masing-masing 92.78 % (ions  $\text{Cu}^{2+}$ ) dan 85.74 % (ion  $\text{Ni}^{2+}$ ) bagi manik kitosan-benzaldehid 1:1 manakala 94.54 % (ion  $\text{Cu}^{2+}$ ) dan 81.55 % (ion  $\text{Ni}^{2+}$ ) bagi manik kitosan-benzaldehid 1:2.

# **ADSORPTION OF Cu(II) AND Ni(II) IONS USING CHITOSAN-BENZALDEHYDE BEADS**

## **ABSTRACT**

Two types of chitosan derivatives, chitosan-benzaldehyde 1:1 and 1:2 beads were prepared and used to adsorb  $\text{Cu}^{2+}$  and  $\text{Ni}^{2+}$  ions from aqueous solution. The beads were characterized using infrared spectroscopy, surface area and pore size analysis and scanning electron microscope coupled with energy dispersive X-ray (SEM-EDX) analysis. The surface charge of the chitosan-benzaldehyde beads was determined by using  $\text{pH}_{\text{pzc}}$ . Batch adsorption studies were carried out to investigate the optimum conditions for the removal of  $\text{Cu}^{2+}$  and  $\text{Ni}^{2+}$  ions using chitosan-benzaldehyde beads for further adsorption studies. Based on thermodynamic studies, the standard enthalpy change ( $\Delta H^\circ$ ) for all the adsorbents were positive indicating an endothermic process. The adsorption of  $\text{Cu}^{2+}$  and  $\text{Ni}^{2+}$  ions by using chitosan-benzaldehyde beads were best described by pseudo-second order kinetic model. The experimental data were best fitted by Freundlich and Redlich-Peterson isotherm model for both chitosan-benzaldehyde 1:1 and 1:2 beads. The maximum adsorption capacity for chitosan-benzaldehyde 1:1 and 1:2 beads were 81.76 and 55.53 mg/g, respectively for  $\text{Cu}^{2+}$  ions and 30.34 and 20.42 mg/g respectively for  $\text{Ni}^{2+}$  ions. For the fixed-bed column studies, the experimental data is well fitted to the both Thomas and Yoon-Nelson models. The percentage of desorption based on desorption studies are 92.78 % for  $\text{Cu}^{2+}$  ions and 85.74 % for  $\text{Ni}^{2+}$  ions when chitosan-benzaldehyde 1:1 beads were used while there was 94.54 % for  $\text{Cu}^{2+}$  ions and 81.55 % for  $\text{Ni}^{2+}$  ions when chitosan-benzaldehyde 1:2 beads were used.

## **CHAPTER ONE**

### **INTRODUCTION**

#### **1.1 Heavy Metals in Our Environment**

Heavy metals pollution is always the challenging environmental problem which needs to be controlled from time to time. This is because heavy metal ions are potentially to cause serious threat to ecosystem and public health due to their toxicity, persistency and bioaccumulation tendency in nature (Wang and Chen, 2014). Exposure to air, water, and soil are all contribute to our uptake of heavy metals. Therefore, proper restriction and legitimates toward the heavy metal disposal should be issued to avoid the excessive heavy metal ions enter our ecosystem.

##### **1.1.1 Copper**

Copper, with symbol Cu and atomic number of 29, is malleable and soft metal with tarnish surface. It turns to brownish colour when exposed to the air. Copper can be found in rock, soil, sediments, water, air as well as animals and plants. Owing to its properties of high thermal and electricity conductivity, copper is an ideal material to be used in electrical industry (Heider et al., 2013). It was applied in printed circuit board manufacturing (Yang et al., 2009), brass manufacturing (Leffers and Ray, 2009), metallurgy (Davenport et al., 2002), electroplating (Yan et al., 2013), paints

(Chen et al., 2013a; Saxena and Dhimole, 2006) and electronics (Raval et al., 2013). Besides, copper also can be used by mix it with other elements. As reported by Dan et al. (2005), the copper implanted stainless steel (also called annealed Cu-implanted) has excellent antibacterial property and good corrosion resistance. Copper ferrite was used to liquefied the petroleum gas (LPG) sensing in petroleum industry at room temperature (Singh et al., 2011). Besides that, copper was applied in agricultural activity as fungicide to protect the plant from fungal diseases attack (Fernández-Calviño et al., 2010; Herrero-Hernández et al., 2011; Zhou et al., 2011). Copper also gained attention as an antimicrobial agent because of its inhibitory effects on bacteria, yeast, and viruses (Ibrahim et al., 2011).

Besides from the contribution in industries and agricultural field, copper also plays an important role in body metabolism. Copper is an essential trace element in performing the enzymatic activity and other functions related to formation of hemoglobin (red blood cells) and synthesis of bone matrix constituent (Heaney, 2001; Shrivastava and Jaiswal, 2013). As proposed by O'Gorman and Humphreys (2012), Cu-Zn superoxide dismutase is responsible for the prevention of antioxidant in the cell. Lu et al. (2006) stated that copper is important in membrane transport functions as it performs specific metabolic function that participate in physiological processes such as respiration, neurotransmitter biosynthesis, radical detoxification and iron intake (Balamurugan and Schaffner, 2006; Richter and Ludwig, 2003; Turley et al., 1997).

However, excessive copper ions in body can be a threat as it is non-biodegradable and tends to bio-accumulate in cells. According to The World Health Organization (WHO), the permissible limit of copper ions in drinking water range from 1 to 5 mg/L (Girgis et al., 2012). Excessive copper ions in body could lead to several

diseases such as vomiting, abdominal pain, nausea (Awual et al., 2013b; Chen et al., 2013b), hemolysis (Hossain et al., 2012), neurological abnormalities and anemia (Awual et al., 2013a; Kumar et al., 2006). Furthermore, the accumulation of copper in different parts of body can cause different diseases. For example, gastrointestinal catarrh and hemochromatosis caused by accumulation of excessive copper ions in liver and kidney (Ajmal et al., 2005; Gündoğan et al., 2004; Gupta et al., 2006; Li et al., 2010b) while inherited Wilson disease (Özlem Kocabaş-Ataklı and Yürüm, 2013; Zhu et al., 2008) caused by excessive copper ions accumulated in tissues. Moreover, copper ions is also a potential carcinogen (Wan et al., 2010). Exposure to unusual high concentration of copper ions in working environment and long term inhalation of copper can cause lung cancer (Aydın et al., 2008; Boujelben et al., 2009; Cheng et al., 2010).

### **1.1.2 Nickel**

Nickel was first discovered by Swedish chemist, Baron Axel Fredrik Cronstedt in 1751. It is malleable silvery white metallic element with atomic number 28, allocated in between cobalt and copper on periodic table. It is fifth most common element on earth, which occurs extensively in the earth's crust. Nickel primarily exists in the 0 and +2 oxidation state (Covington et al., 1985). Most of the world's supply of nickel is mined in Sudbury Basin of Ontario, Canada. Nickel occurs occasionally free in nature, but mainly in ore as laterite (oxide and silicates) and sulphites. Nickel laterite ore is one of the primary source of nickel which contributes to about 70% of world

land based nickel resources (Mazinanian et al., 2013). Due to the properties of corrosion resistance, better toughness and better strength at high and low temperature, nickel is applied to various industry activities such as textile and paint industry, foundries and metal finishing industry (Vinod et al., 2010), electroplating, smelting, batteries manufacturing, forging, textile dyeing and leather tanning (Mubarok and Lieberto, 2013). Besides, nickel also widely applied in alloy manufacturing. For example, zinc–nickel alloy electrodeposits were used to substitute toxic cadmium coatings due to its properties of excellent corrosion resistance, low hydrogen brittleness and high chemical stability (Qiao et al., 2012). As like copper, nickel also one of the essential metallic micronutrient in our body. Enzyme needs nickel to speed up chemical reactions such as ureolysis, hydrogen metabolism, methane biogenesis and acidogenesis (Akhtar et al., 2004).

However, only trace amount of nickel are needed in our body, excessive uptaken of nickel will caused health deterioration. According to World Health Organization (WHO), the permissible concentration of nickel in drinking water is less than 0.1 mg/L (Duman and Ayranci, 2010). Overdosing of nickel can cause acute poisoning such as headache, nausea, chest pain, tightness of the chest, dry cough and breath difficulty (Kandah and Meunier, 2007; Olgun and Atar, 2012). Besides the acute poisoning, excessive of nickel can cause nasopharynx, lung and dermatological diseases as well as malignant tumors (Hadi et al., 2013). Long term period expose to nickel can cause skin allergy. This is normally happened to people whose wearing jewels containing nickel alloy or to the workers whose exposed to nickel-rich products (Kandah and Meunier, 2007). Nickel also posses the carcinogen nature. The most reported cancer were lung, nasal sinus, (Wang et al., 2007) bone and nose

cancer (Kwon and Jeon, 2013; Hasar, 2003). Besides the nickel itself, nickel compounds also has detrimental effect on human health (Wang et al., 2007; Wang et al., 2009c). According to Sun et al. (2009) and Li et al. (2009b), nickel compounds have been associated with respiratory cancer, human kidney cells mutations and also in alteration of epigenetic homeostasis. The carcinogenic nickel carbonyl can be easily absorbed by skin (Vieira et al., 2010). The exposure of this compound at atmospheric concentration of 30 mg/L for half an hour can caused fatality while acute exposure to nickel carbonyl can cause pulmonary fibrosis and renal edema (Sadeghi et al., 2011).

## **1.2 Treatment Technology for Heavy Metals Containing Wastewater**

Inadequate access to safe and clean water can cause serious global health problem. Contaminations of water by heavy metals are harmful to biological organisms and also to the environment. Thus, it is necessary to effectively and deeply remove the toxic heavy metals from water system before it was discharging the treated into natural bodies of water. To date, several techniques have been introduced in order to remove the heavy metal ions from wastewater. Among them are chemical precipitation, ion exchange, membrane separation, electrochemical methods (electrocoagulation and electroflotation) and adsorption.

### 1.2.1 Chemical precipitation

Chemical precipitation is one of the techniques used to remove the heavy metal ions from wastewater. This technique involves the conversion of heavy metal ions into insoluble solid (fine and colloidal particles form) after reacted with precipitating agent in wastewater system. The precipitated solid will then be removed by using settling, filtration and membrane techniques. This method is widely applied in acid mine drainage, neutral drainage and pit lake water. Heavy metal ions can be precipitate from wastewater as hydroxide, sulphides, or carbonates.

Hydroxide precipitation involves the formation of insoluble metal hydroxide when alkaline agents such  $\text{Ca(OH)}_2$  (lime),  $\text{NaOH}$  (caustic),  $\text{CaO}$ ,  $\text{Mg(OH)}_2$  or  $\text{NH}_4\text{OH}$  were added to the metal-laden wastewater (Djedidi et al., 2009). Lime is always be the selected precipitant because of its lowest cost among the precipitants (Lee et al., 2007). The chemical reaction involved in the hydroxide precipitation formation are as following (Oncel et al., 2013):



In sulfide precipitation, heavy metal ions reacted with sulphides ions to form solid sulphide. There are several sulfides used in the sulphide precipitation such as  $\text{FeS}$  (s),  $\text{CaS}$  (s),  $\text{Na}_2\text{S}$  (aq),  $\text{NaHS}$  (aq),  $\text{NH}_4\text{S}$  (aq),  $\text{H}_2\text{S}$  (g) and  $\text{Na}_2\text{S}_2\text{O}_3$  (Lewis, 2010). The chemical reaction involved in sulphide precipitation formation was described as following:





Both the  $HS^{-}$  and  $S^{2-}$  resulted from the dissociation of added  $H_2S$  and hydrolysis of sulphide salt. The insoluble metal sulphide has low solubility over a broad range of pH and precipitation of selective heavy metal ions by using sulphide are possible at very low pH (Feng et al., 2000; Villa-Gomez et al., 2011). Moreover, the stability of metal sulfide sludges produced is higher than corresponding hydroxide and carbonate sludge. This is because the dewatering and thickening characteristic of sulphide is much more better than the corresponding hydroxide and carbonate sludges (Velasco et al., 2008).

Alternatively, inorganic carbonates were added for the precipitation to occur. Inorganic carbonates that usually used as the reagent are  $NaHCO_3$ ,  $CaCO_3$ , and  $Na_2CO_3$ . The chemical reaction involved in formation of insoluble metal carbonates was described as following:



The low solubility of metal carbonates has always made it a good approach to get rid of heavy metal ions from wastewater (Ouhadi et al., 2011).

### **1.2.2 Ion exchange technique**

Ion exchange involves the exchange of same amount of charged ions from solution with equal amount of similarity charged ions attached to ion exchange resin (Abdelwahab et al., 2013; Abo-Farha et al., 2009). This technique is highly selective for ions even in very low concentration (Badawy et al., 2009; Feng et al., 2000). The polymer resin used in ion exchange device made up of either naturally occurring mineral or synthetically material. An example of naturally occurring mineral material is zeolite. Zeolite is highly selective for certain metal ion and can be found abundantly on earth (Çoruh et al., 2010; Jovanovic et al., 2012). The cage-like structure provides countless of cavities and pores and this resulted in large surface area available for ion exchange to take place (Mozgawa et al., 2009). Nevertheless, synthetically material is preferred over the naturally occurring mineral material for its higher efficiency and lower cost.

Ion exchange resin can be classified into two main groups: cation and anion exchange resin. The exchangeable ions attached on cation and anion exchange resin are positive and negative ions respectively. The functional groups attached onto cation exchange resin could be sulfonic acid groups (Amara and Kerdjoudj, 2002; Gehrke et al., 1996; Sahu et al., 2009), carboxylic groups (Littlejohn and Vaughan, 2012; Mori et al., 2006; Riveros, 2004), phosphonic groups and phosphinic groups (Alyüz and Veli, 2009) whereas the functional groups attached on anion exchange resin could be ammonium groups (Dicinoski et al., 2000; Marsh et al., 1997; Wołowicz and Hubicki, 2009; Yoon et al., 2009), polyamine groups (Donia et al.,

2011; Gode and Pehlivan, 2005; Miyazaki and Nakai, 2011; Pehlivan and Cetin, 2009) and nitrogen heterocycle groups (Marinho et al., 2011). Ion exchange technique has been employed for the treatment of wastewater by many researchers. For example, Pehlivan and Altun (2007), Rao et al. (2010) and Rengaraj et al. (2001) proposed that the ion exchange resin showed high removal ability on  $Pb^{2+}$ ,  $Cu^{2+}$ ,  $Zn^{2+}$ ,  $Cd^{2+}$ ,  $Ni^{2+}$  and  $Cr^{3+}$  ions from wastewater.

### **1.2.3 Membrane separation**

Owing to high driving forces and transport selectivity of membrane (Mortaheb et al., 2010; Ulbricht, 2006), membrane technology has received a considerable attention for the treatment of wastewater released from variety of industry operation processes. This technology utilized a membrane which is semi-permeable as a barrier between the solutions which only selective permeate solute in the solution is allowed to pass through. Most of the semi-permeable membranes are made of polymer and inorganic materials (Negrão Murakami et al., 2011). This technique not only applied in the separation of heavy metal ions but also the separation of dyes and organic pollutant. Generally, there are four separation methods: microfiltration (MF), ultrafiltration (UF), nanofiltration (NF) and reverse osmosis (Chougui et al., 2014).

Pressure-driven membrane process in microfiltration (MF) utilizes a membrane with pore sizes of 0.02 to 10  $\mu m$ . Any organic or inorganic molecule that is smaller than this membrane sizes are allowed to permeate through (Ramirez and Davis, 1998; Tomasula et al., 2011). Several applications of microfiltration in the removal of

hazardous heavy metal ions from the wastewater have been studied. Broom et al. (1994) investigated the industrial wastewaters containing toxic heavy metals by using microfiltration while Jana et al. (2010) using low-cost ceramic microfiltration membrane for the removal of chromate from aqueous solution.

Ultrafiltration (UF) is usually used to retain colloidal, suspended particulate and high molecular weight compound (1000 to 100000 Da) from permeate through the membrane (Arthanareeswaran et al., 2007; Nagendran et al., 2008). Pore sizes of the membrane utilized in ultrafiltration is lies between 5 to 20 nm (Barakat, 2011). To enhance the performance of the ultrafiltration, the membrane was cast with water soluble polymers. By doing this, the heavy metal will formed large size complex when associated with the polymer. The complexes will forbid from passing through the selective membrane. Normally used water soluble polymers are polyacrylic acid (PAA), polyethyleneimine (PEI), polyvinylalcohol (PVA), polyacrylic acid sodium salt (PAASS) and poly(dimethylamine co-epichlorohydrin-co-ethylene-diamine) (PDEHED) (Cojocar et al., 2009). According to Barakat and Schmidt (2010), the application of this technique in the wastewater containing  $\text{Cu}^{2+}$ ,  $\text{Ni}^{2+}$ ,  $\text{Cr}^{3+}$  had resulted in high percentage of metal ions removal.

The separation by nanofiltration (NF) was established by the middle of eighties after the developed of reverse osmosis in seventies (Van der Bruggen and Vandecasteele, 2003). To date, nanofiltration is still become the most preferred technology in wastewater treatment (Cissé et al., 2011). The molecular weight cut-off (MWCO) of nanofiltration membrane is ranging from 200-1000 Da which is lies between the membrane characteristic of ultrafiltration (UF) and reverse osmosis (RO) (Rundel et al., 2007). This technology can effectively reject any organic or inorganic pollutants

which has larger sizes than the pore size of the membrane (1-5 nm) (Zahrim and Hilal, 2013). The retention ability of membrane also depends on electrical charge on the surface and steric hindrance present in the solution (Abidi et al., 2011; Hesampour et al., 2010). Some researches regarding to heavy metal ions removal by using nanofiltration (NF) have been proposed. For example, Al-Rashdi et al. (2013) proposed that by using nanofiltration membrane, the  $\text{Cu}^{2+}$ ,  $\text{Cd}^{2+}$ ,  $\text{Mn}^{2+}$  and  $\text{Pb}^{2+}$  ions were effectively removed from wastewater whereas in Otero et al. (2012) work, they revealed that high percentage of rejection of Cr (VI) (> 95 %) was achieved.

Reverse osmosis is a pressure-driven process which involves the application of pressure into the system in order to attain the desirable permeable production rate (Bartman et al., 2009; Hollman and Bhattacharyya, 2003). The dense semi-permeable reverse osmosis membrane allows only the passage of water but not large molecule, ions ( $\text{Na}^+$ ,  $\text{Ca}^{2+}$ ,  $\text{Cl}^-$ ), microorganisms, colloids, dissolved salts and organic (Abejón et al., 2012) to pass through. The salt or compound retained will be collected for further treatment (Pérez-González et al., 2012).

#### 1.2.4 Electrocoagulation

Electrochemical treatment involves the plating-out of heavy metal ions on cathode surface and then recovers metals in the elemental metal state (Fu and Wang, 2011). The common used electrochemical techniques in wastewater treatment are electrocoagulation (EC) and electroflotation (EF). In electrocoagulation (EC) process, the active coagulant (destabilisation agent) (Emamjomeh and Sivakumar, 2009) was generated in situ when an external potential was passing through the aqueous medium (Mouedhen et al., 2008) with Al or Fe as anode (sacrificial electrode). During the process (when current is passing through), water molecule and metal anode were reduced and oxidized to  $\text{OH}^-$  ions and  $\text{Al}^{3+}$  ions ( $\text{Fe}^{3+}$  if Fe as anode) simultaneously. The  $\text{Al}^{3+}$  will then react with  $\text{OH}^-$  ions to form polyvalent polyhydroxide complex (hydroxide floc) (Aber et al., 2009). The possible hydroxide floc generated by  $\text{Al}^{3+}$  are  $\text{Al}(\text{OH})_2^{2+}$ ,  $\text{Al}_2(\text{OH})_2^{4+}$ ,  $\text{Al}(\text{OH})_4^-$ ,  $\text{Al}_6(\text{OH})_{15}^{3+}$ ,  $\text{Al}_7(\text{OH})_{17}^{4+}$ ,  $\text{Al}_8(\text{OH})_{20}^{4+}$ ,  $\text{Al}_{13}\text{O}_4(\text{OH})_{24}^{7+}$  and  $\text{Al}_{13}(\text{OH})_{34}^{5+}$  (Trompette and Vergnes, 2009) whereas  $\text{Fe}^{3+}$  will produce hydroxide floc such as  $\text{Fe}(\text{H}_2\text{O})_6^{3+}$ ,  $\text{Fe}(\text{H}_2\text{O})_5(\text{OH})^{2+}$ ,  $\text{Fe}(\text{H}_2\text{O})_4(\text{OH})_2^+$ ,  $\text{Fe}_2(\text{H}_2\text{O})_8(\text{OH})_2^{4+}$  and  $\text{Fe}_2(\text{H}_2\text{O})_6(\text{OH})_4^{4+}$  (Daneshvar et al., 2007). These positively charged complexes possessed high affinity to coagulate with pollutants to form aggregates after neutralized the negative charge on the surface of the colloids particles (Phalakornkule et al., 2010). This technique was used by Akbal and Camcı (2011) to remove copper, chromium, and nickel from metal plate wastewater. The results showed that 100 % of copper, chromium, and nickel were removed at an EC time of 20 min, a current of  $10 \text{ mA/cm}^2$  and a pH of 3.0. Besides, the performance of EC process with Al electrodes in the treatment of copper, zinc

and manganese containing aqueous solution was investigated by Hanay and Hasar (2011). Total removal of copper and zinc reached almost 100 % after 5 min at pH value >7 whereas the manganese removal percentage were 85% (in the presence of sulfate) and 80 % (in the presence of chlorine anion) respectively.

### **1.2.5 Electroflotation**

Electroflotation (EF) was first proposed by Elmore in 1904. This technique was applied in the separation of certain mineral from ore by the floating principle (Chen, 2004). The floating species could be solids, heavy metal ion, macromolecules, fibers or any particles present in the wastewater. EF process operates when an external current was applied to contaminated wastewater system consisting of two electrodes (Mansour et al., 2007). When current is passing through, the water molecule in the solution will reduced to H<sub>2</sub> gas at cathode and oxidized to O<sub>2</sub> gas at anode simultaneously (Casqueira et al., 2006). The pollutants in the solution will adhere on these tiny bubbles to form floc and then float upward until it reached to the water surface. As time passed, these pollutant-containing bubbles will gradually concentrated and form a layer of foam that can be skimmed away easily later on (Koren and Syversen, 1995). There are few studies were done on the performance of EF. Oussedik and Khelifa (2001) proposed that 90 % of Cu<sup>2+</sup> ions had been successfully removed from the galvanoplastic industry wastewater. Khelifa et al. (2005) found that Ni, Cu, Zn and Co reached 98-99 % of removal when EF technique was applied in the metal finishing effluents treatment.

### **1.2.6 Adsorption technique**

Adsorption is one of the equilibrium separation methods used to treat heavy metal laden-effluents. This technique is the mostly used technique in wastewater treatment to date because of its advantages of low cost, simple design of operation and no harmful by-product produced during the process (Chatterjee et al., 2010). This technique not only applied to eliminate the metal ions but also organic pollutants, colloidal substance, dyes, odor, and sediments. During the adsorption, the desired particles will adhere or concentrated onto the surface area of adsorbent through the attraction force (van der Waals forces). Under an optimum condition, adsorption can give highest efficiency in removing the pollutants (Foo and Hameed, 2010).

Adsorbent plays an important role in determining the heavy metal ions removal efficiency and the stability of an adsorption process. It is a substance used to absorb the desired particles from aqueous solution onto its surface or interface (Ali et al., 2012; Bhatia et al., 2009). Activated carbon is one of the high efficiency adsorbent used in the adsorption system. However, the high cost of the activated carbon has limited its contribution in wastewater treatment. Therefore, a search for low-cost adsorbent is necessary. Natural adsorbents are high demanding adsorbent among the adsorbents due to the low-cost and effective characteristic in treating the heavy metal ions. Natural adsorbents can be classified into four groups: agricultural waste, clay minerals, algae biomass and microbial biomass. Agricultural waste is the most interest as it is abundantly available and environmental friendly. Besides, it is economic and suitable for the adsorption process that required a lot of adsorbents. The next interesting natural adsorbent was clay. Clay minerals can be obtained easily

from landfill and underground. It is also an important composition in manufacturing of building material and ceramic. Together with the increasing understanding and researching on its structural and composition, it was found that clay has special inherent potential of excellent sorption capability. Clay is widely used in adsorption process to substantially eliminate heavy metal ions from the aqueous solution (Addy et al., 2012). Algae biomass is one of the adsorbent used to remove heavy metal ions. There are many studies was done on the heavy metal ions removal by using algae biomass. Most of the results were promising and this shows that algae biomass will become the largest and widely used adsorbent in the future. Microbial biomass also used in the removal of inorganic pollutants nowadays. Microbial biomass adsorbent is the bacteria that involved in the biosorption of heavy metal. Table 1.1 has listed some examples of natural adsorbents together with the heavy metal ions adsorbed.

Table 1.1 Summary of type of natural adsorbents used in removal of heavy metal

Type of adsorbents	Adsorbents	Metal ions	References
Agriculture waste	Orange juice residue	Cu(II) Pb(II) Fe(II) Cd(II) Zn(II) Mn(II)	Dhakal et al. (2005)
	Oil palm shell	Cu(II) Pb(II)	Chong et al. (2013)
	Rice husk	Cr(VI) Cu(II) Pb(II) Fe(II) Mn(II) Zn(II) Cd(II)	Chuah et al. (2005)
	Peanut hull pellets	Cu(II) Cd(II) Zn(II) Pb(II)	Brown et al. (2000)
	Spent grain	Cu(II) Pb(II) Zn(II) Cd(II)	Li et al. (2010a)
	Oak sawdust	Cu(II) Ni(II) Cr(IV)	Argun et al. (2007)
	Chestnut shell	Cu(II) Pb(II) Zn(II)	Vázquez et al. (2009)
	Tea waste	Cr(VI)	Ng et al. (2013)

	Pigeon peas hulls powder	Pb(II) Ni(II)	Venkata Ramana et al. (2012)
	Oyster shell powder	Cu(II) Ni(II)	Hsu (2009)
Clay	Montmorillonite	Hg(II) Pb(II) Cu(II) Ni(II) Mn(II) Cd(II)	De Pablo et al. (2011)
	Kaolin	Cu(II)	Wang et al. (2009b)
	Clinoptilolite rock	Cd(II) Cu(II) Pb(II) Cr(IV) Ni(II)	Sprynskyy et al. (2007)
	Palygorskite	Pb(II) Cr(VI) Cu(II) Ni(II)	Potgieter et al. (2006)
	Sepiolite	Co(II) Cu(II) Zn(II) Cd(II) Pb(II)	Brigatti et al. (2000)
	Illite	Cu(II) Zn(II)	Turan et al. (2011)
	Smectite	Zn(II)	Mhamdi et al. (2013)
	Vermiculite	Cd(II) Cu(II) Pb(II)	Vieira dos Santos and Masini (2007)
	Rectorite	Zn(II)	Zhang et al. (2005)

---

Algae biomass	<i>Ecklonia maxima</i>	Cd(II) Cu(II) Pb(II)	Feng and Aldrich (2004)
	<i>Fugus species</i>	Cd(II)	Herrero et al. (2006)
	<i>Ulvalactuca</i>	Cr(VI)	El-Sikaily et al. (2007)
	<i>Laminaria japonica</i>	Ni(II) Cu(II)	Liu et al. (2009)
	<i>Spirogyra species</i>	Cu(II) Pb(II)	Gupta and Rastogi (2008); Rajfur et al. (2012)
	<i>Gracilariaverrucosa</i>	Cr(VI)	Ata et al. (2012)
	<i>Ulvafasciata species</i>	Zn(II)	Prasanna Kumar et al. (2007)
	<i>Durvillaea antarctica</i>	Pb(II)	Hansen et al. (2013)
	<i>Fucus serratus</i>	Cu(II)	Ahmady-Asbchin et al. (2008)
	<i>Ulothrix cylindricum</i>	As(III)	Tuzen et al. (2009)
	<i>Chaetomorpha linum</i>	Cu(II) Zn(II)	Ajjabi and Chouba (2009)
Microbial biomass	<i>Bacillus strain CR-7</i>	Cu(II) Zn(II)	Xu et al. (2011)
	<i>Citrobacter species</i>	Pb(II) Zn(II)	Puranik et al. (1999)
	<i>Geobacillus thermodenitrificans</i>	Fe(III) Cr(III) Co(II)	Chatterjee et al. (2010)

---

## **1.3 Chitin**

### **1.3.1 Source of chitin**

Chitin is the second most abundant polysaccharide in biomass after cellulose (Hajji et al., 2014). The structure of chitin is similar to that of cellulose except for or C-2, which acetyl group instead of hydroxyl group is bounded (Akkaya et al., 2009) (Figure 1.1). Chitin is one of the valuable element in shell of shrimp, prawn, crab, lobster, crayfish and krill (Nicol and Hosie, 1993). It is responsible for the formation of protective exoskeletons and peritrophic membranes in arthropods (Doucet and Retnakaran, 2012). Besides that, chitin also act as essential structural components in forming cell walls in fungi and yeast (Dotto et al., 2013; Schleuter et al., 2013).

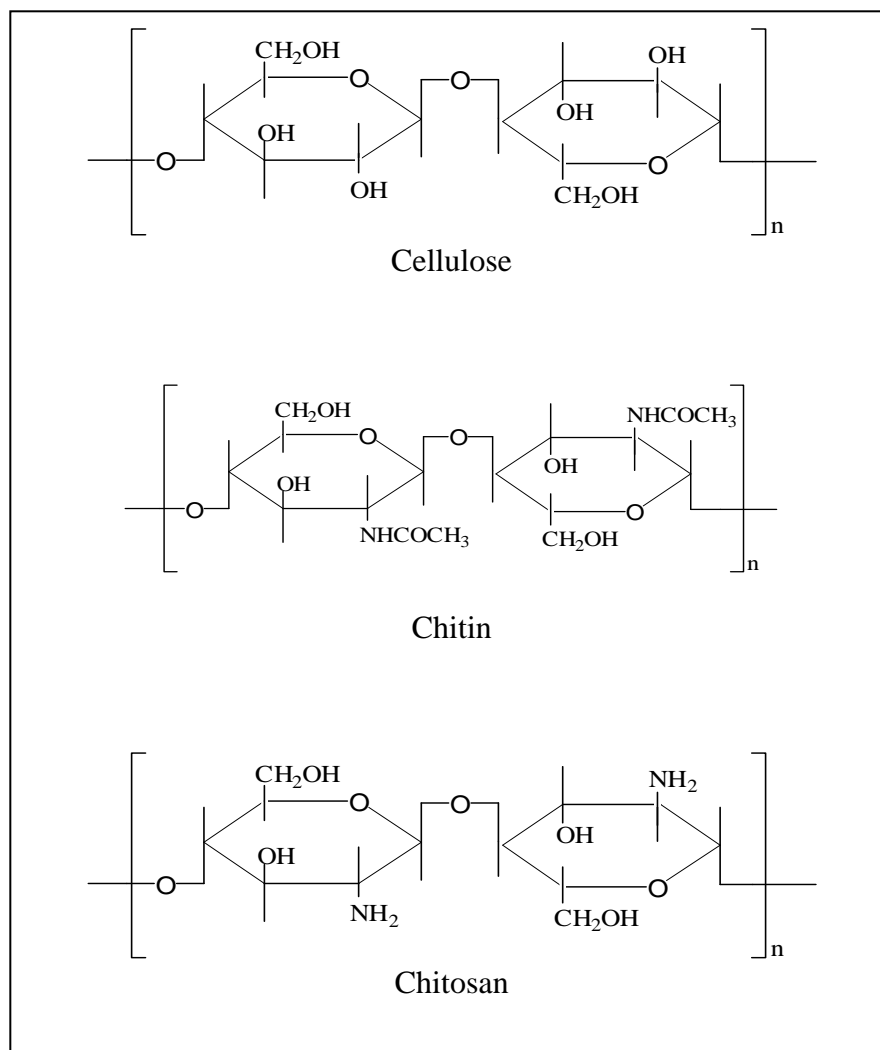


Figure 1.1 Structures of cellulose, chitin and chitosan (Krajewska, 2004)

### 1.3.2 Properties of Chitin

Chitin is a polymer with structure of  $\beta$ -(1,4)-linked N-acetyl-D-glucosamine. It is non-toxic, biodegradable, biocompatible and antibacterium natural polymer. It has high potential in heavy metal ions removal. This could be attributed to the high

hydrophilicity and high chemical reactivity which resulted from large number of functional groups. Besides, chitin is extremely insoluble in water and certain organic solvent due to its rigid crystalline structure (Hajji et al., 2014). However, chitin still can be dissolved by using dissolution reagent such as hexafluoro isopropanol, hexafluoroacetone, dimethylacetamide containing 5 % lithium chloride and chloroalcohols in conjugation with aqueous solutions of mineral acids. Besides that, the mixture of formic acid and dichloroacetic acid, trichloroacetic acid and dichloroethane, dimethylacetamide and lithium chloride, methane sulfonic acid, calcium chloride dihydrate saturated methanol, and 10 % sodium hydroxide solution also can be used to dissolve chitin (Aiba, 2001).

## **1.4 Chitosan**

### **1.4.1 Propertise of chitosan**

Chitosan, a long chain natural polycationic polymer with repeated structure of  $\beta$ -(1,4)-linked D-glucosamine (Zhou et al., 2010) is the product of the deacetylation of chitin in an alkaline or acidic medium (Figure 1.1). There are one protonated amino and two hydroxylic groups (chelating groups) available in each unit of chitosan chain. These functional groups are responsible in binding with metal ions. Chitosan poses the same advantages as chitin: non-toxicity, hydrophilicity, biocompatibility and biodegradability (Wan Ngah et al., 2011). It exhibits antifungal and antimicrobial activity to against bacteria and fungi (Qin et al., 2006; Ziani et al., 2009). In the aspect of solubility, the presence of highly hydrophobic groups in the structure had

contributed to the characteristic of non-solubility in the water. Yet, the protonation of amino functional groups of chitosan had caused it to be soluble in acid medium. Chitosan can be available in different molecular weight and degree of deacetylation which depending on the source and the processing technique. It is reported that chitosan has molecular weight ranging from 300 to 1000 kDa while the degree of deacetylation available is range from 30 to 90 % (Islam et al., 2014).

## **1.5 Application of Chitosan**

Considering of its unique physiochemical characteristics, chitosan is applicable widely in many fields. Among them are textiles (Sye et al., 2008), food (Dutta et al., 2009), agriculture (El-Sawy et al., 2010), medical (Aiba, 2001) and wastewater industry.

### **1.5.1 Textile industry**

The application of chitosan in fabric treatment for the purpose of textile quality improvement has been widely studied. Several studies showed that chitosan able to improve the shrinkage and dyeing behavior of textiles. According to Pascual and Julià (2001), the treatment with chitosan on wool fabrics showed that the shrinkage resistance increased when higher viscosity of chitosan was used whereas the dyeing process is favorable when lower viscosity chitosan was applied. Chattopadhyaya and

Inamdarb (2013) proposed that the dyeing ability of nano-chitosan treated cotton towards direct dye is improved. The increased dye uptake due to chitosan treatment was attributed to the presence of primary amino groups of chitosan. These cations dissipate the negative surface charge on cotton and drive the dye molecule to the fiber.

Besides its contribution on the shrinkage and dyeing of textile, chitosan also acts as antimicrobial agents in textile industry. It is well known that the hydrophilic porous structure and moistures transport characteristic of textile which made from fiber and cellulose are highly requires protection from microbial. Therefore, uses of microbial agent are very important to keep textile away from the harmful bacteria. As reported by Alonso et al. (2009), the textile made by the chitosan cross-linked cellulose fibers showed significantly decreases of *Escherichia coli* (kind of bacteria) on the textile as compared to the untreated cellulose fiber textile. Lim and Hudson (2004) treated the cotton with *O*-acrylamidomethyl-*N*-[(2-hydroxy-3-trimethylammonium)propyl] chitosan chloride (NMA-HTCC) at a concentration of 1 % on weight of fabric and the result showed 100 % of bacterial reduction. Liu et al. (2013a) evaluated the antibacterial activity on the fabric by using patchouli oil embedded chitosan-gelatin microcapsules. The antibacterial rate of the fabrics for *Staphylococcus aureus* and *Escherichia coli* were about 65 % even after being washed 25 times.

### **1.5.2 Food industry**

Owing to the properties of anti-microbial, anti-oxidized and non-toxicity (Jung and Zhao, 2014), chitosan was used as food preservative. Chitosan is known to be the effective natural preservative for meat. It can effectively prevent the microbial spoilage and inhibit the lipid oxidation (which were the causes of the meat deterioration) (Chantararataporn et al., 2014). According to Kanatt et al. (2008), the use of mint and chitosan in meat products is well suited to improve the shelf life and safety of meat and other fresh foods. Besides the raw meat, chitosan also coated upon the cooked meat to preserve its freshness. This has been revealed by Kanatt et al. (2013) who proposed that chitosan coating can retain the good quality, improve the freshness (microbiological safety) and extend ready-cook-meat shelf life during the chilled storage.

Besides that, chitosan also used as coating for the shelf-life extension of fruits and vegetables (Devlieghere et al., 2004; Gol et al., 2013). Dong et al. (2004) showed that application of chitosan coating can be effectively maintain the quality and extend the shelf life of peeled fruit. Chien et al. (2007) proposed that coating citrus fruit exhibited greater antifungal resistance and its quality can be maintained for longer time. Xing et al. (2011) revealed that quality of sweet peppers can be maintained for 35 days at 8 Celsius after applied the chitosan-oil coating upon the sweet peppers. Besides its role as food preservative, the non-toxic, anti-bacterial and excellent film-forming property of chitosan had made it a suitable choice as packaging in food industry. The study performed by Cruz-Romero et al. (2013) on the antibacterial activity of chitosan and nano-sized solubilisates in potential food